$XeNO_3^+$: A Gaseous Cation Characterized by a Remarkably Strong Xe−O Bond

Fernando Bernardi,[†] Fulvio Cacace,[‡] Giulia de Petris,*[,‡] Federico Pepi,[‡] and Ivan Rossi[†]

Dipartimento di Chimica "G. Ciamician", Università di Bologna, via Selmi, 2, 40126 Bologna, Italy, and Dipartimento di Studi di Chimica e Tecnologia delle Sostanze Biologicamente Attive, Università di Roma "La Sapienza", p.le A. Moro, 5, 00185 Rome, Italy

Received: January 14, 1998; In Final Form: April 21, 1998

The joint application of experimental techniques, such as MIKE, CAD, and FT-ICR spectrometry, and computational methods (DFT and QCISD(T)) has allowed preparation and characterization of gaseous $XeNO_3^+$ and $XeNO_2^+$ ions. The most stable structure of $XeNO_3^+$ has the $XeONO_2$ connectivity, with a relatively short (2.088 Å) Xe−O bond, and represents the gas-phase counterpart of Xe(II) nitrate, previously observed in solution. The $XeNO_2^+$ cation is best characterized as a $[Xe-NO_2]^+$ complex, with a large (3.018 Å) Xe−NO_2 separation and a relatively low dissociation energy, 10.8 kcal mol^{-1}. The reaction of $XeNO_3^+$ with selected nucleophiles, including CH_3OH, $C_2H_5NO_2$, CH_3COCH_3, CH_3CN, and C_2H_5CN, investigated by FT-ICR mass spectrometry, characterizes the ion as a nitrating agent. The unimolecular and collision-induced fragmentation of $XeNO_3^+$ and $XeNO_2^+$ is discussed.

Introduction

Since the discovery of noble gas reactivity,[1] a number of compounds of XeF_2 with strong fluoride ion acceptors have been synthesized.[2−5] In particular, Lewis acids such as AsF_5, SbF_5, and RuF_5 have been found to enhance the ionic character of the Xe−F bond through the formation of the corresponding XeF_2MF_5 and $XeF_2M_2F_{10}$ adducts, where the XeF^+ cation has been well characterized by spectroscopic methods. Both the saltlike and the fluorine-bridged formulations of these Xe(II) species show the XeF^+ cation as having a significant Lewis-acid strength. Numerous examples of bonding with organic and inorganic basic centers, involving Xe−N,[6−9] Xe−C,[10,11] and Xe−O[12,13] bonds, have been characterized in the solid state and in solution.

By contrast, the ion chemistry of the XeF^+ cation has not been investigated in depth in the gas phase. The estimated electron affinity of XeF^+, 10.9 eV, [9] suggests that a number of Lewis bases, resistive to its oxidative attack, could react with the XeF^+ cation, according to addition and/or displacement processes. Here we present an experimental and theoretical study of the structure of new Xe(II) species, namely, the $XeNO_3^+$ and the $XeNO_2^+$ ions, prepared for the first time in the gas phase and characterized by mass spectrometric and theoretical techniques. In particular, the reaction of XeF^+ with nitric acid, occurring in the HNO_3/XeF_2 chemical ionization (CI) plasma, has been identified as the most convenient route to $XeNO_3^+$ and is investigated in depth.

Experimental Section

All chemicals were research-grade products from Aldrich Chemical Co. and were used without further purification. Ozone was synthesized by passing UHP-grade oxygen (Matheson 99.95%) through a commercial ozonizer. Dinitrogen pentoxide was synthesized by the method of Davidson at al.,[14] involving oxidation of NO by O_3. All gases used were purchased from Matheson Gas Products Inc. with a stated purity in excess of 99.95 mol %. MIKE spectra were recorded using a ZAB-2F mass spectrometer from VG Micromass Ltd. and represent the average of at least 30 scans. The kinetic energy release was measured at an energy resolution of 5000 fwhm. The CAD spectra were aquired by using He as collision gas. The FT-ICR experiments were performed utilizing a 47e Apex mass spectrometer from Bruker Spectrospin AG, equipped with an external ion source, operated at total pressures not exceeding 7×10^{-5} Torr. The triple-quadrupole (TQ) experiments were performed using a Model Quattro instrument from VG Micromass Ltd. The ions produced in the ion source were mass-selected in the first quadrupole (Q1) and introduced into the reaction cell (a radio frequency only hexapole) containing the neutral reagent at pressures up to 10^{-4} Torr. The translational energy of the ions was approximately 0.5 eV (laboratory frame).

Mass Spectrometric Results

$[Xe,N,O_3]^+$ Ions. The CI spectrum of neat XeF_2 is strongly affected by the pressure. At the relatively high pressure typical of the ZAB CI source (0.05−0.1 Torr), the CI spectra display XeF^+ as the base peak, together with Xe^+ (31%), XeF_2^+, Xe_2F^+, $Xe_2F_2^+$ (≅10% each), and $Xe_2F_3^+$ (70%) ions. The XeF_2/CI of HNO_3 yields $XeNO_3^+$ ions having the expected isotopic pattern, most likely from the reaction of HNO_3 with fluorinated cations, since $XeNO_3^+$ ions are not formed by Xe/CI of HNO_3. Confirmation of this hypothesis has been sought by utilizing TQ mass spectrometry. One isotopomer of the most likely precursor, the $^{129}XeF^+$ ion, has been mass-selected in the first quadrupole of the TQ spectrometer and driven into the second quadrupole, containing HNO_3. The observation of the ^{129}Xe-NO_3^+ product ion unambiguously demonstrates the occurrence of the reaction

$$XeF^+ + HNO_3 \rightarrow XeNO_3^+ + HF \qquad (1)$$

Having established the formation pathway of $XeNO_3^+$, the ion has been generated in the source of a reverse geometry mass

[†] Università di Bologna.
[‡] Università di Roma "La Sapienza".

S1089-5639(98)00781-6 CCC: $15.00
Published on Web 06/24/1998

TABLE 1: Fragmentation Pattern of $XeNO_3^+$ and $XeNO_2^+$ Ions

fragment *m/z*	intensity (%Σ) $XeNO_3^+$ [a] source of ion reaction 1	reaction 2	$XeNO_2^+$ [a]
	MIKE Spectra		
175	75.5	79.8	
62	21.6	16.5	
46	2.9	3.6	100
	CAD Spectra		
145	40.9	43.0	
129	55.3	53.5	95.5
30	3.8	3.5	4.5

[a] The spectra are referred to the $^{129}XeNO_3^+$ and $^{129}XeNO_2^+$ precursor ions. The same results are obtained from $^{131}XeNO_3^+$ and $^{131}XeNO_2^+$, $^{132}XeNO_3^+$ and $^{132}XeNO_2^+$. [b] Peaks having a metastable contribution have been excluded.

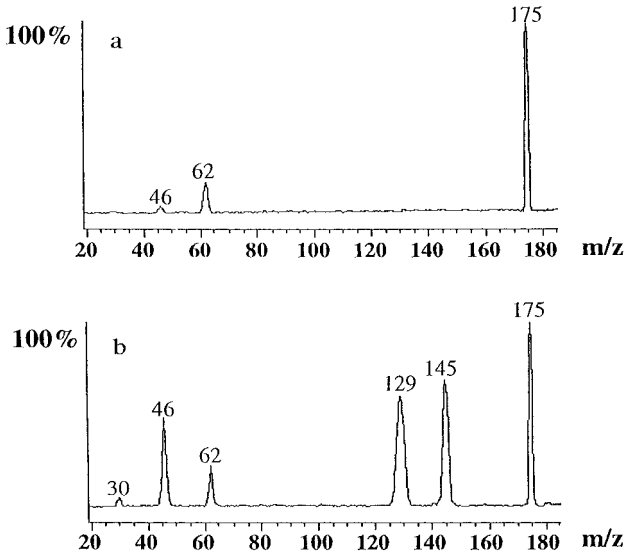

Figure 1. MIKE (a) and CAD (b) spectra of $^{129}XeNO_3^+$ ion from reaction 1.

spectrometer, and the most abundant isotopomers, $^{129}XeNO_3^+$, $^{131}XeNO_3^+$, and $^{132}XeNO_3^+$, have been structurally assayed by mass analyzed kinetic energy (MIKE) and collisionally activated dissociation (CAD) spectrometry. The MIKE spectrum of each precursor ion shows the corresponding $XeNO_2^+$ and NO_3^+ fragments, with but a small percentage of NO_2^+. The CAD spectra display, in addition, significant abundances of the XeO^+ and Xe^+ fragments (Table 1). $XeNO_2^+$, the major fragment in the MIKE spectrum, appears as a very sharp peak (Figure 1), and furthermore its small kinetic energy release, $T_{0.5} = 19.9 \pm 0.9$ meV, does not appreciably increase following collision-induced dissociation ($T_{0.5} = 27.9 \pm 1.6$ meV).

An alternative route to $XeNO_3^+$ ions involves XeO^+, the most abundant ion formed in the chemical ionization of a gaseous Xe/O_3 mixture. In the presence of dinitrogen pentoxide the displacement process

$$XeO^+ + N_2O_5 \rightarrow XeNO_3^+ + NO_3 \qquad (2)$$

occurs, and the $XeNO_3^+$ ions formed display the same spectral features as those of the ions from reaction 1, as shown in Table 1.

Reactions 1 and 2 have been studied in the external CI ion source of a FT-ICR mass spectrometer, operated at pressures up to 10^{-5} Torr, their charged products being unambiguously identified by accurate mass measurements extended to a number of isotopomers containing ^{129}Xe, ^{131}Xe, ^{132}Xe, and ^{134}Xe. The $XeNO_3^+$ ions prepared in the external source have been driven into the resonance cell and allowed to react with a number of nucleophiles, Nu, to gather structurally informative reactivity data. As shown in Table 2, the NO_2^+ ion transfer is the most significant reaction, provided that the Nu has a sufficient NO_2^+/BE.[15] When the ligand-exchange reaction is energetically unfavorable, charge transfer can be observed, whose occurrence and extent depend on the ionization potential of the nucleophile.[16] Competing charge exchange and NO_2^+ ion transfer are observed when both processes are energetically allowed within the reaction complex, due to the comparable ionization potentials of nucleophile and NO_2, as exemplified when Nu = CH_3COCH_3.

TABLE 2: Reactivity of $XeNO_3^+$ Ion toward Selected Nucleophiles as a Function of Their NO_2^+/BE and IP

Nu	NO_2^+/BE[a] (kcal mol^{-1})	IP[a] eV	reaction
C_2H_5CN	26.5	11.84	NO_2^+ transfer
CH_3COCH_3	25.9	9.70	NO_2^+/charge exchange[b]
CH_3CN	25.5	12.19	NO_2^+ transfer
$C_2H_5NO_2$	24.0	10.88	NO_2^+ transfer
CH_3OH	21.5	10.85	no reaction
H_2O	19.6	12.61	no reaction
HCl	(11.1)[c]	12.75	no reaction
NO	(10.4)[c]	9.26	charge exchange[b]

[a] All the NO_2^+/BE and IP data are from refs 15 and 16, respectively. [b] When observed, the charge exchange is highly efficient. [c] The values in parentheses are obtained from the PA−NO_2^+/BE correlation reported in ref 15. The PA of NO is taken from ref 17.

[Xe,N,O$_2$]$^+$ Ions. $XeNO_2^+$ ions have been generated by nitration of xenon, conveniently performed by N_2O_5/Xe/CI. Their MIKE and CAD spectra, reported in Table 1, display a simple dissociation into Xe^+ and NO_2^+ fragments. Remarkably, attempts at generating $XeNO_2^+$ ions by addition of XeO^+ to nitric oxide under CI conditions have proved unsuccessful.

Computational Results

A computational study of the structures and the energetics associated with the experimentally detected $XeNO_3^+$ and $XeNO_2^+$ ions has been performed, by using an approach based on the density functional theory. The computational method used is the nonlocal density functional known as BLYP[18,19] coupled with the local spin density-optimized DZVP basis set.[20,21] The geometries of the various stationary points have been fully optimized with the gradient method, and their nature has been determined by computing the harmonic vibrational frequencies. Thermochemical corrections have been calculated too. All the calculations have been performed using the Gaussian-94 program.[22] The binding energies (BEs) of some cluster species have been calculated taking into account the correction for the basis set superposition error (BSSE) by means of the counterpoise[23,24] procedure, which includes fragment relaxation energy terms.[25−27]

Three structures have been found that correspond to minima on the potential energy surface of $XeNO_3^+$ (see Figure 2a for geometrical parameters). From the energy data shown in Table 3, the most stable structure, labeled **M1**, shows a Xe−O−NO_2 connectivity, like a nitric acid molecule whose hydrogen atom has been replaced by xenon. Two structural features are salient, namely, the strained bond between the nitrogen and the bridging oxygen atom, and the relatively short Xe−O bond distance,

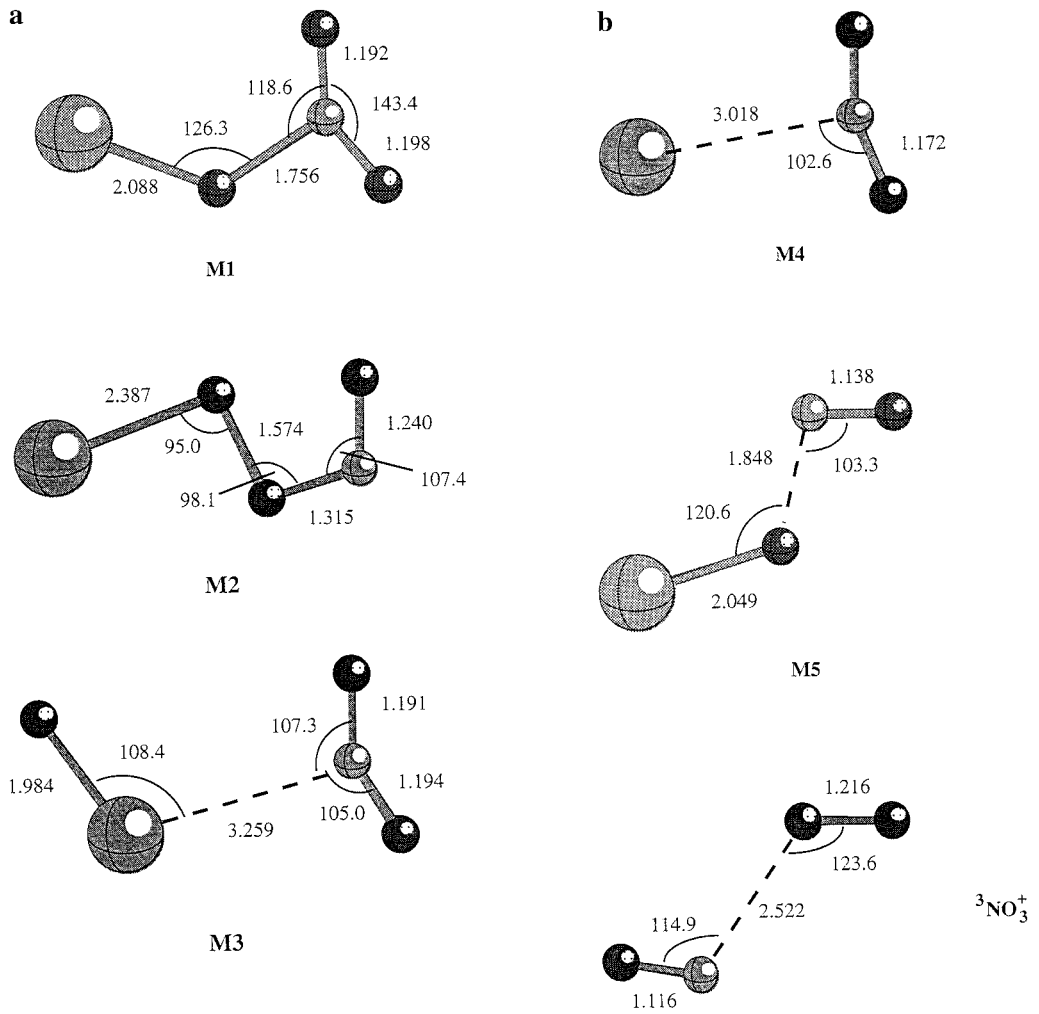

Figure 2. (a) Optimized geometries of species relevant to $XeNO_3^+$. (b) Optimized geometries of species relevant to the $XeNO_2^+$ and NO_3^+ systems.

TABLE 3: BSSE-Corrected Absolute and Relative Energies (*E*) and Enthalpies (*H*) at 0 and 298 K for $XeNO_3^+$ and $XeNO_2^+$ at the BLYP/DZVP Level.

	E		*H* (0 K)		*H* (298 K)	
	(au)	(kcal/mol)	(au)	(kcal/mol)	(au)	(kcal/mol)
$[XeNO_3]^+$						
M1	−7513.911 204	0.0	−7513.898 038	0.0	−7513.891 559	0.0
M2	−7513.865 092	28.9	−7513.853 258	28.1	−7513.846 785	28.1
M3	−7513.856 642	34.2	−7513.845 297	33.1	−7513.837 751	33.8
$XeO + NO_2^+$	−7513.830 828	50.4	−7513.818 715	49.8	−7513.814 099	48.6
$XeO^+ + NO_2$	−7513.830 671	50.5	−7513.823 811	46.6	−7513.816 423	47.1
$Xe + {}^3NO_3^+$	−7513.942 427	−19.6	−7513.932 915	−21.9	−7513.924 045	−20.4
$Xe^+ + NO_3$	−7513.844 656	41.8	−7513.835 241	39.4	−7513.828 432	39.6
$[XeNO_2]^+$						
M4	−7438.784 361	0.0	−7438.773 980	0.0	−7438.768 334	0.0
M5	−7438.728 047	35.3	−7438.719 644	34.1	−7438.713 781	34.2
$Xe + NO_2^+$	−7438.767 479	10.6	−7438.757 194	10.5	−7438.751 163	10.8

which approaches the range (1.8−2.0 Å) typical of covalently bound Xe atoms. The two other isomers **M2** and **M3** lie ca. 28 and 34 kcal mol^{-1} higher in energy than **M1** and are characterized by much larger Xe−O and Xe−N bonds (Figure 2a). Table 4 reports the calculated $\Delta H°$ of reactions 1 and 2, for isomer **M1**.

The stability of **M1** with respect to the heterolytic and homolytic fragmentations of the xenon−oxygen and the bridging oxygen−nitrogen bonds has also been investigated, the fragmentation into Xe and triplet NO_3^+ being identified as an exothermic dissociation. The triplet NO_3^+ species is actually a very weakly bound cluster of NO^+ with a dioxygen molecule, since its calculated binding energy is very close to zero at the most reliable level used (QCISD(T)/6-311G*).[27,29] Despite the use of the BSSE correction, the BLYP approach appears to substantially overestimate the stability of this cluster (Table 5).

TABLE 4: Absolute Energies (*E*) and Enthalpies (*H*) at 0 and 298 K for $XeNO_3^+$ (isomer M1) Formation from Reactions 1 and 2 Calculated at the BLYP/DZVP Level

	E (au)	*H* (0 K)	*H* (298 K) (au)
$XeF^+ + HNO_3$	−7794.145818	−7794.119988	−7794.108756
$XeNO_3^+ + HF$	−7794.196610	−7794.171988	−7794.161059
Δ (kcal/mol)	−31.87	−32.63	−32.82
$XeO^+ + N_2O_5$	−7614.322905	−7614.297007	−7614.288901
$XeNO_3^+ + NO_3$	−7614.362457	−7614.340536	−7614.330752
Δ (kcal/mol)	−24.82	−27.31	−26.26

TABLE 5: BSSE-Corrected Absolute and Relative Energies (*E*) and Enthalpies (*H*) at 0 and 298 K for the $^3NO_3^+$ Binding Energy at the BLYP/DZVP and the QCISD(T)/6-311G*//BLYP/DZVP Levels

		E		*H* (0 K)		*H* (298 K)	
		(au)	(kcal/mol)	(au)	(kcal/mol)	(au)	(kcal/mol)
$NO^+ + {}^3O_2$	BLYP	−279.899 904	0.0	−279.891 315	0.0	−279.888 010	0.0
	QCISD(T)	−279.364 953	0.0	−279.356 364	0.0	−279.353 059	0.0
$^3NO_3^+$	BLYP	−279.929 043	−18.3	−279.919 531	−17.7	−279.913 020	−15.69
	QCISD(T)	−279.368 665	−2.3	−279.359 153	−1.8	−279.352 642	0.3

TABLE 6: BSSE-Corrected Absolute and Relative Energies (*E*) and Enthalpies (*H*) at 0 and 298 K for XeO Atomization Energy at the BLYP/DZVP Level

	E		*H* (0 K)		*H* (298 K)	
	(au)	(kcal/mol)	(au)	(kcal/mol)	(au)	(kcal/mol)
$Xe + {}^3O$	−7309.085 549	0.0	−7309.085 549	0.0	−7309.080 831	0.0
XeO	−7309.076 733	5.5	−7309.072 932	7.9	−7309.071 988	5.5

The heterolytic fragmentation of the bridging oxygen−nitrogen bond generates the xenon oxide neutral molecule. Despite being a bound state characterized by a 549 cm^{-1} stretching frequency, it is only kinetically stable, since its atomization into ground-state xenon and oxygen atoms is computed to be exothermic (see Table 6).

The two **M4** and **M5** minima identified on the potential energy surface of $XeNO_2^+$, shown in Figure 2b, correspond to a Xe−nitronium ion cluster and to a nitrosonium−xenon oxide cluster. **M4** appears to be largely more stable than **M5** with a NO_2^+/BE energy of 10.8 kcal mol^{-1} at 298 K (see Table 3).

Discussion

Formation of $XeNO_3^+$. The XeF^+ cation is a strong Lewis acid, whose positive charge is mostly localized on the xenon atom. Accordingly, early electrostatic association to HNO_3 is expected to yield a $[FXe- - -O(H)NO_2]^+$ cluster, rapidly evolving into the products, namely, the $XeNO_3^+$ ion and HF, the high stability of the latter providing the driving force to the whole process:

$$XeF^+ HNO_3 \rightarrow [FXe---O(H)NO_2]^+ \rightarrow XeONO_2^+ + HF \quad (4)$$

It is interesting to note that related reactions involving nitrates and highly fluorinated compounds have been described in solution.[30]

$$XeF_n + MNO_3 \rightarrow MF + [F_{(n-1)}\,XeONO_2] \rightarrow F_{(n-2)}\,XeO + FNO_2 \quad (5)$$

The mechanism suggested to account for the generally observed formation of the MF and FNO_2 products involves a putative intermediate $F_{(n-1)}XeONO_2$, which undergoes a facile internal nucleophilic substitution, followed by FNO_2 elimination.

Whereas the gaseous $[FXe- - -O(H)NO_2]^+$ intermediate has not been detected in this study, support for the mechanism outlined in reaction 4 is lended by the following considerations. When performing the reaction with a simple nitric acid derivative, methyl nitrate, the $[FXe- - -O(CH_3)NO_2]^+$ adduct has actually been observed as a product of the reaction

$$XeF^+ + CH_3ONO_2 \rightarrow [FXe---O(CH_3)NO_2]^+ \quad (6)$$

Its MIKE spectrum shows a single transition,

$$[FXe---O(CH_3)NO_2]^+ \rightarrow XeOCH_3^+ + FNO_2 \quad (6a)$$

corresponding to the $XeOCH_3^+$ ion, consistent with an initial Xe−O connectivity, followed by the loss of the best leaving group, HF or FNO_2, depending on whether a proton is available, according to the scheme.

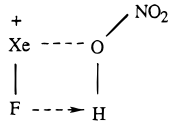

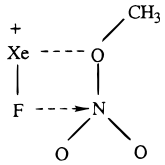

By analogy, the mechanism postulated for reaction 1 argues for the formation of a product suggestive of the $XeO-NO_2$ connectivity of the isomer denoted **a**. As to reaction 2, the isomer **b**, having an $OXe-NO_2$ connectivity, is likely the primary product, although formation of isomer **a** cannot be excluded.

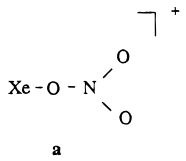

a

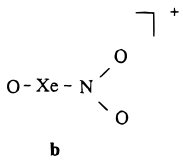

b

Structural Analysis of $XeNO_3^+$ Populations. As a whole, the experimental results concur in outlining a picture where the same $[Xe,N,O_3]^+$ ionic population is detected in the 10 μs time frame of MIKE and CAD spectrometry. At first glance, irrespective of the formation process, the metastable NO_3^+ and $XeNO_2^+$ fragments seem to reflect the connectivity typical of isomers **a** and **b**, respectively. However, a salient feature of the experimental picture, and in our opinion the key for the interpretation of mass spectrometric results, is the remarkably small kinetic energy release, in the fragmentation into $XeNO_2^+$, which clearly occurs at, or very near to, the threshold. Isomer **a** is not a likely parent for the following reasons: (i) it does not contain a preformed Xe−N bond and hence extensive rearrangement would be required, (ii) loss of an oxygen atom from the nitro group is expected to be highly endothermic and to involve anyhow a reverse activation barrier, which would entail an appreciable kinetic energy release. A larger than observed release would be expected as well from a parent having the connectivity typical of ion **b**, due to the O−Xe single-bond cleavage. In other words, the small kinetic energy release observed seems inconsistent with the fragmentation of covalently bonded structure, falling instead in the range usually assigned to the dissociation of weakly bound adducts.

Comparison with Theoretical Results. The structures characterized as true minima by the theoretical calculations are

SCHEME 1

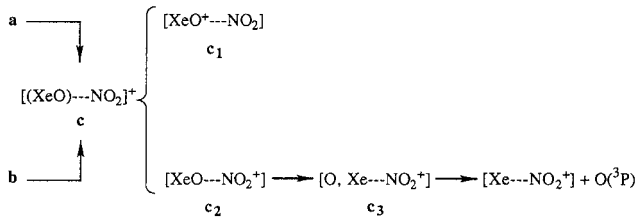

all satisfactorily consistent with the experimental evidence. The **M1** and **M3** minima, whose stability difference is calculated to amount to 33.8 kcal mol^{-1}, show the connectivity assigned to the ions denoted **a** and **b**, respectively. Nevertheless, on the basis of the theoretically computed exothermicities of reactions 1 and 2 (Table 4), isomer **b** (**M3**) could be formed only from the reaction 2. As a consequence, the experimental evidence pointing to a single $XeNO_3^+$ population, irrespective of the way of formation, would rule out $XeNO_3^+$ precursor ions having the **b** connectivity. On the other hand, the fragmentation pattern of the $XeNO_3^+$ ions is not typical of covalently bound species such as **a** or **b**, being rather more consistent with the dissociation of an ion−neutral complex. In fact, ions **a** (**M1**) having a large energy excess can undergo a fission of the strained O−N bond, so that the bond joining XeO and NO_2 moieties can be broken, the two species remaining nevertheless electrostatically associated, within an ion−molecule complex. A similar fission can conceivably occur from isomers **b** (**M3**), whose formation from reaction 2 is energetically possible. In fact, even displaying the connectivity typical of **b**, the **M3** structure can be most appropriately described as a cluster, whose weakest bond is the Xe−N bond. The frequency of the Xe−N bond stretching in ion **b** (**M3**) has been calculated, and the computational results lead to a value of ca. 245 cm^{-1}. This suggests a very weak bond and hence dissociation of **b** (**M3**) ions containing just a small excess of internal energy. The result is that, within a certain range of excess internal energy below the dissociation threshold, both isomers **a** (**M1**) and **b** (**M3**), can lose their initial connectivity, evolving into an electrostatic complex $[(XeO)- - -NO_2]^+$, denoted as **c**.

As shown in Scheme 1, the positive charge can reside on both the XeO (cluster $\mathbf{c_1}$) and the NO_2 (cluster $\mathbf{c_2}$) groups, since their ionization potentials have been estimated to be very close.[31] When $\mathbf{c_2}$ is formed, the unstable XeO molecule dissociates, and the Xe atom becomes the neutral ligand, forming a $[O, Xe- - -NO_2^+]$ cluster (see later). It is clear from the foregoing that the intermediacy of the ternary complex $\mathbf{c_3}$ would satisfactorily explain the remarkably small kinetic energy release observed, typical of very weakly bound adducts such as $\mathbf{c_3}$, formed by the $[Xe- - -NO_2^+]$ moiety associated with an extremely poor ligand such as the oxygen atom. This hypothesis provides, in addition, a reasonable explanation for the otherwise surprising observation that the kinetic energy release increases only by a few meV following collisional activation. In fact, the large internal energies typical of the collisional excitation step fall well above the restricted range, allowing formation of the very weakly bound complex $\mathbf{c_3}$. Finally, direct fragmentation to NO_2^+, competing with that to $[Xe- - -NO_2^+]$, accounts for the small peak of NO_2^+ observed in the MIKE spectra.

Dissociation of the most stable isomer **a** (**M1**) to the most stable NO_3^+ ion, a $[O_2- - -NO^+]$ cluster, is predicted to be energetically allowed (Table 3). The NO^+/BE of O_2 computed at the BLYP level amounts to 15.7 kcal mol^{-1} (Table 5), a far larger value than the experimental one of 2.9 kcal mol^{-1}.[33] A calculation performed at a higher level of theory (QCISD(T)/6-311G*//BLYP/DZVP) gives a NO^+/O_2 BE in much better agreement with the experimental value (Table 5), pointing to the limitations attached to the density functional theory in this specific application. In fact, the DFT results reported in this paper are expected to be accurate when they compare similar species, as in the case of the relative energies of bonded species between themselves or the relative energies of separated species between themselves. The accuracy is admittedly lower when they are computed dissociation energies, which include energies of bonded species and dissociated species. Based on the theoretically predicted exothermicity of the fragmentation of $XeNO_3^+$ ion into Xe and NO_3^+ within the metastable-ion time window, an entropic bottleneck to the decomposition has to be expected. Actually, given the structures of isomer **a** (**M1**) and of the NO_3^+ ion (Figure 2b), such a barrier is likely, since extensive rearrangement is required in order to reach the appropriate critical configuration for the formation of the $[NO^+- - -O_2]$ complex. A better candidate would be represented by the **M2** ion, less stable than **a** (**M1**) by ca. 28 kcal mol^{-1}, but no experimental evidence for this isomer has been obtained. Neverthless, as mentioned before, ions **a** (**M1**) are generated with a large energy excess, and the level of the **M2** minimum on the potential energy surface can be taken as indicative of the internal energy content required for ion **a** (**M1**) to reach the appropriate configuration to decompose into NO_3^+.

FT-ICR Evidence. The ICR evidence shows that NO_2^+ transfer from $XeNO_3^+$ ions occurs only to ligands whose NO_2^+/BE exceeds a certain threshold; that is, NO_2^+ transfer to CH_3CN (NO_2^+/BE = 24 kcal mol^{-1}) but not to CH_3OH (NO_2^+/BE = 21.5 kcal mol^{-1}) is observed, which sets the threshold around ≅23 kcal mol^{-1}. This in turn suggests that the NO_2^+/BE in the nitrating species must be lower than ≅23 kcal mol^{-1}. Clearly based on the theoretical results (Table 3), NO_2^+ transfer from ion **a** would be energetically unfavorable to all ligands investigated,[15] even considering contribution from the energetically favorable dissociation of XeO. This is an interesting observation, in that calculations based on the theoretically computed enthalpy changes combined with the available experimental data on the heats of formation of relevant neutrals[16] allow a rough estimate of the NO_2^+/XeO BE in complex **c**, which happens to be 24 ± 5 kcal mol^{-1}, not inconsistent with the threshold deduced from the FT-ICR experiments.[32a]

Structure of $XeNO_2^+$ Ions. The MIKE and CAD spectra of the $XeNO_2^+$ ions from the nitration of xenon suggest the structure of a $[Xe- - -NO_2^+]$ complex, which corresponds to the most stable minimum (**M4**) on the potential energy surface (Figure 2). No evidence has been obtained for the less stable $XeONO^+$ ion (**M5**). The experimental failure to detect $[Xe,N,O_2]^+$ ions from the addition of XeO^+ to nitric oxide can point to the occurrence of charge transfer, further favored by the subsequent fast and exothermic dissociation of XeO, or to the excessive exothermicity of the reaction.[32b] The ions formed can dissociate out of the metastable-ion time window or isomerize to the most stable structure, much above the dissociation threshold, which would explain the failure to detect any $[Xe,N,O_2]^+$ products from the addition of XeO^+ to NO.

Conclusive Remarks

In conclusion, the most stable $XeNO_3^+$ ion shows a nitric acid-like structure, where a hydrogen is replaced by a xenon atom, susceptible to being effectively transferred to a suitable ligand. Since we have been unable to exploit formation processes less exothermic than reactions 1 and 2, the mass spectrometric results reflect the large internal energy content

of the $XeNO_3^+$ ions formed. Unavoidably, a fraction of their population loses the initial $XeO-NO_2$ connectivity, evolving into an electrostatic $[(XeO)NO_2]^+$ complex. The most stable species among $XeNO_2^+$ ions has the ion−molecule structure, probably due to the relatively large polarizability of Xe, which makes the atom a relatively good ligand of NO_2^+. Furthermore, charge exchange does not occur, being prevented by the largely unfavorable ΔIP difference. Further studies of the reactivity of XeF^+ toward a number of selected nucleophiles are in progress, in these laboratories. Finally, it is interesting to note that a neutral species, $Xe(ONO_2)_2$, formally a Xe(II) salt, is known in solution as a product from the reaction of XeF_2 with a HNO_3/NO_2 mixture.[34] In light of this, the $XeONO_2^+$ cation observed in the gas phase may be regarded as a Xe(II) mononitrate.

Acknowledgment. The financial support from the Rome University "La Sapienza" and Consiglio Nazionale delle Ricerche (CNR) is gratefully acknowledged. The authors are indebted to F. Angelelli for FT-ICR measurements and to Prof. M. Attinà for TQ experiments.

References and Notes

(1) Bartlett, N. *Proc. Chem. Soc. (London)* **1962**, 218.

(2) Edwards, A. J.; Holloway, J. H.; Peacock, R. D. *Proc. Chem. Soc.* **1963**, 275.

(3) Cohen, B.; Peacock, R. D. *J. Inorg. Nuclear Chem.* **1966**, *28*, 3056; McRae, V. M.; Peacock, R. D.; Russel, D. R. *Chem. Commun.* **1969**, 62.

(4) Sladky, F. O.; Bulliner, P. A.; Bartlett, N.; DeBoer, B. G.; Zalkin, A. *Chem. Commun.* **1968**, 1048. Binenboym, J.; Selig, H.; Shamir, J. *J. Inorg. Nucl. Chem.* **1968**, *30*, 2863.

(5) Holloway, J. H.; Knowles, J. G. *J. Chem. Soc. (A)* **1969**, 756. Bartlett, N.; Gennis, M.; Gilber, D. D.; Morrel, B. K.; Zalkin, A. *Inorg. Chem.* **1973**, *12*, 1717.

(6) LeBlond, R. D.; DesMarteau, D. D. *J. Chem. Soc. Chem., Commun.* **1974**, 555. Sawyer, J. F.; Schrobilgen, G. J.; Sutherland, S. J. *Inorg. Chem.* **1982**, *21*, 4064.

(7) Emara, A. A. A.; Schrobilgen, G. J. *J. Chem. Soc., Chem. Commun.* **1987**, 1644. Schrobilgen, G. J. *J. Chem. Soc., Chem. Commun.* **1988**, 1506.

(8) Emara, A. A. A.; Schrobilgen, G. J. *J. Chem. Soc., Chem. Commun.* **1988**, 257.

(9) Emara, A. A. A.; Schrobilgen, G. J. *Inorg. Chem.* **1992**, *31*, 1323.

(10) Frohn, H. J.; Jakobs, S. *J. Chem. Soc., Chem. Commun.* **1989**, 625.

(11) Zhdankin, V. V.; Stang, P. J.; Zefirov, N. S. *J. Chem. Soc., Chem. Commun.* **1992**, 578. Frohn, H. J.; Klose, A.; Henkel, G. *Angew. Chem., Int. Ed. Engl.* **1993**, *32*, 99.

(12) Bartlett, N.; Wechsberg, M.; Sladky, F.; Bulliner, P. A.; Jones, G. R.; Burbank, R.D. *Chem. Commun.* **1969**, 703. Sladky, F. *Angew. Chem.* **1969**, *81*, 536. McKee, D. E.; Adams, C. J.; Bartlett, N. *Inorg. Chem.* **1973**, *12*, 1722.

(13) Olah, G. A.; Chambers, R. D.; Prakash, G. K. S. In *Synthetic Fluorine Chemistry*; Wiley: New York, 1992.

(14) Davidson, J. A.; Viggiano, A. A.; Howard, C. J.; Dotan, I.; Fehesenfeld, F. C.; Albriton, D. L.; Ferguson, E. E. *J. Chem. Phys.* **1978**, *68*, 2085.

(15) Cacace, F.; de Petris, G.; Pepi, F.; Angelelli, F. *Proc. Natl. Acad. Sci. U.S.A.* **1995**, *92*, 8635.

(16) Lias, S. G.; Bartmess, J. E.; Liebman, J. F.; Holmes, J. L.; Levin, R. D.; Mallard, W. G. *J. Phys. Chem. Ref. Data* **1988**, 17, Suppl. 1.

(17) Kuo, S.-C.; Zhang, Z.; Ross, S. K.; Klemm, R. B.; Johnson, R. D., III; Monks, P. S.; Peyton Thorn Jr., R.; Stief, L. J. *J. Phys. Chem.* **1997**, *101*, 4035.

(18) Becke, A. D. *Phys. Rev.* **1988**, *38*, 3098.

(19) Lee, C.; Yang, W.; Parr, R. G. *Phys. Rev.* **1988**, *37*, 785.

(20) Godbout, N.; Salahub, D. R.; Andzelm, J.; Wimmer, E. *Can. J. Chem.* **1992**, *70*, 560.

(21) DZVP Xe basis set was obtained from the Extensible Computational Chemistry Environment Basis Set Database, Version 1.0, as developped and distributed by the Molecular Science Computing Facility, Environmental and Molecular Sciences Laboratory, which is part of the Pacific Northwest Laboratory, P.O. Box 999, Richland, WA 99352. Web address: http://www.emsl.pnl.gov:2080/forms/basisform.html.

(22) Frisch, M. J.; Trucks, G. W.; Schlegel, H. B.; Gill, P. M. W.; Johnson, B. G.; Robb, M. A.; Cheeseman, J. R.; Keith, T.; Petersson, G. A.; Montgomery, J. A.; Raghavachari, K.; Al-Laham, M. A.; Zakrzewski, V. G.; Ortiz, J. V.; Foresman, J. B.; Cioslowski, J.; Stefanov, B. B.; Nanayakkara, A.; Challacombe, M.; Peng, C. Y.; Ayala, P. Y.; Chen, W.; Wong, M. W.; Andrés, J. L.; Replogle, E. S.; Gomperts, R.; Martin, R. L.; Fox, D. J.; Binkley, J. S.; Defrees, D. J.; Baker, J.; Stewart, J. P.; Head-Gordon, M.; Gonzales, C.; Pople, J. A. *Gaussian94*, Revision D.3; Gaussian, Inc.: Pittsburgh, PA, 1995.

(23) Boys, S. F.; Bernardi, F. *Mol. Phys.* **1970**, *19*, 553.

(24) For a recent review on the subject see: van Duijneveldt, F. B.; van Duijneveldt, J. G. C. M.;. van Lenthe, J. H *Chem. Rev.* **1994**, *94*, 1873.

(25) Emsley, J.; Hoyte, O. P. A.; Overill, R. E. *J. Am. Chem. Soc.* **1978**, *100*, 3303.

(26) Smith, P. H.; Derissen, J. L.; van Duijneveldt, F. B. *J. Chem. Phys.* **1978**, *69*, 521.

(27) Xantheas, S. S. *J. Phys. Chem.* **1996**, *100*, 8821.

(28) Pople, J. A.; Head-Gordon, M.; Raghavachari, K. *J. Chem. Phys.* **1987**, *87*, 5968.

(29) Krishnan, R.; Binkley, J. S.; Seeger, R.; Pople, J. A. *J. Chem. Phys.* **1980**, *72*, 650.

(30) Wilson, W. W.; Christe, K. O. *Inorg. Chem.* **1987**, *26*, 916. Christe, K. O.; Wilson, W. W. *Inorg. Chem.* **1988**, *27*, 1296.

(31) The ionization potential of XeO has been evaluated from a thermochemical cycle, utilizing the computed endothermicities of the dissociation of **a** (**M1**) into $XeO(XeO^+)$ and into NO_2^+ (NO_2). All other thermochemical values are taken from ref 16.

(32) (a) The theoretically computed enthalpy changes given in Tables 3−6, combined with available experimental heats of formation (ref 16), allow the heat of formation of $XeNO_3^+$ ion **a** (**M1**) to be estimated via different thermochemical cycles. Comparison of the different results obtained from this admittedly rough approach shows a large error bar, ±5 kcal mol^{-1}, due to the combination of theoretical and experimental uncertainties. From the $H_f°$ of $[Xe- - -NO_2]^+$, obtained from the computed NO_2^+/BE of Xe, it is possible to evaluate the endothermicity of the decomposition of $XeNO_3^+$ into $XeNO_2^+$, amounting to ca. 24 ± 5 kcal mol^{-1}. Assuming that the fragmentation occurs near the threshold from the complex **c**, one can estimate that the complex **c** is correspondingly less stable than isomer **a** (**M1**) and ca. 24 kcal mol^{-1} below the dissociation threshold into XeO and NO_2^+. (b) The addition of XeO^+ to NO can be evaluated from the data above (ref 31) ca. 60 kcal mol^{-1} exothermic with respect to the less stable isomer **M5**.

(33) Hiraoka, K.; Yamabe, S. *J. Chem. Phys.* **1991**, *95*, 6800.

(34) Eisenberg, M.; DesMarteau, D. D. *Inorg. Nucl. Chem. Lett.* **1970**, *6*, 29.